IOP Publishing Measurement Science and Technology
Meas. Sci. Technol. 26 (2015) 105901 (7pp) doi:10.1088/0957-0233/26/10/105901

Validation of a calibration set-up for radiosondes to fulfil GRUAN requirements

H Sairanen, M Heinonen and R Högström

VTT Technical Research Centre of Finland Ltd—Centre for Metrology MIKES, PO Box 1000, FI-02044 VTT, Finland

E-mail: hannu.sairanen@vtt.fi

Received 4 May 2015, revised 24 July 2015
Accepted for publication 24 July 2015
Published 26 August 2015

Abstract

Interest in the precise measurement of water vapour in the upper-air is growing along with the consciousness of climate change. Because better knowledge of high altitude humidity levels improves the accuracy of climate models and weather forecasts, the Global Climate Observing System (GCOS) is putting more effort into the quality of these measurements. The GCOS established the Reference Upper-Air Network (GRUAN) and set the requirements for its measurements accuracy and traceability to the International System of Units (SI). To fulfil these requirements, improved radiosondes and methods to calibrate them are being developed. This paper presents a new calibration system for radiosondes based on mixing air flows from two independent dew-point generators. The system operates in the air temperature range down to −80 °C. Our results show that the new calibration set-up is able to provide calibrations for radionsondes at the uncertainty level of 2% in terms of the water vapour mixing ratio as required by GRUAN. A complete calibration covering the whole temperature and humidity range lasts less than three days. Additionally, the apparatus provides an option to characterize the behaviour of a radiosonde in changing temperatures and water vapour concentrations.

Keywords: radiosonde, calibration, GRUAN, humidity, traceability, uncertainty

(Some figures may appear in colour only in the online journal)

1. Introduction

Climate change studies and weather forecast models require accurate measurement data from the upper atmosphere along with data from ground stations. So far the measurement data from the upper-air do not meet the quality level demanded by the Global Climate Observing System (GCOS). To improve the quality of the data, the GCOS launched the Reference Upper-Air Network (GRUAN), which specifies requirements for upper-air measurements and thus aims at improving the quality of data in terms of traceability to the International System of Units (SI) and accuracy (GCOS 2013).

GRUAN has identified water vapour pressure as one of the most important measurands and has set an accuracy requirement of 2% in terms of the mixing ratio. Also, the relevant measurement range was specified from 0.1 ppm_v to 90000 ppm_v (GCOS 2007), which corresponds to a dew/frost-point temperature range from −90 to 44 °C. Moreover, radiosondes should be calibrated in terms of humidity at different temperatures down to −80 °C covering the range encountered in the upper troposphere and stratosphere.

As the ranges of water vapour pressure and air temperature relevant for a radiosonde are wide, several humidity points at several temperatures are needed to be included in a calibration scheme to obtain appropriate reliability. Therefore, a calibration set-up capable of quick changes in humidity is necessary for keeping the calibration time at a reasonable level. Using a traditional single-pressure humidity generator a humidity calibration of a radiosonde takes at least one week. To achieve faster operation, a novel calibration set-up was developed comprising a measurement chamber optimized for GRUAN requirements fulfilling reference radiosondes (Lakka *et al* 2013) and a generator system based on a hybrid humidity generator (HHG) principle (Meyer *et al* 2008). The concept of the system was introduced in (Sairanen *et al* 2014).

This paper presents the constructed calibration apparatus operating in a temperature range from −80 to 20 °C and a dew/frost-point temperature range from −90 to 10 °C. A thorough

validation was performed for the single components, i.e. saturator, zero-air heat exchanger and measurement chamber, and for the complete system. Based on the validation, a full uncertainty budget was drawn up for the system. As an operational test, the apparatus was applied for calibrating a prototype of Vaisala's reference radiosonde RR01. The work was carried out at VTT Technical Research Centre of Finland Ltd—Centre for Metrology (MIKES) and within the MeteoMet projects of the European Metrology Research Programme (EMRP).

2. Theory

GRUAN prioritized water vapour pressure as one of the key parameters in upper-air measurements. However, the accuracy requirement for water vapour pressure was set in terms of the mixing ratio. According to Dalton's law, the partial pressure of water vapour in air (e_w) equals the water vapour amount fraction (x_w) multiplied by the air pressure (p)

$$e_w(t_d)f(p, t_d) = x_w p. \quad (1)$$

Because humid air is not an ideal gas, an enhancement factor (f) is introduced in equation (1) to correct effects caused by interaction between water molecules and air components. The enhancement factor depends on the pressure and dew-point temperature (t_d). In this work, the enhancement factor and the water vapour saturation pressure are calculated according to Hardy (1998) and Sonntag (1998), respectively.

When operating with a HHG, two air flows with different water vapour concentrations are mixed. The water vapour amount fraction of the mixed air flow is calculated according to equation (2) derived from equation (1):

$$x_w = \frac{\dot{m}_{G1}}{\dot{m}_{G1} + \dot{m}_{G2}} \frac{e_{wG1} f_{G1}}{p_{G1}} + \frac{\dot{m}_{G2}}{\dot{m}_{G1} + \dot{m}_{G2}} \frac{e_{wG2} f_{G2}}{p_{G2}}. \quad (2)$$

In equation (2) subscripts G1 and G2 identify the inlet air flows and $\dot{m}$ stands for the mass flow rate. To meet the requirements of GRUAN, we calculate the mixing ratio (r_w) using the well-known relationship:

$$r_w = \frac{x_w \frac{M_w}{M_g}}{1 - x_w}. \quad (3)$$

In equation (3) M_w and M_g are the molecular masses of water and air, respectively. The molar masses are obtained from Wieser (2006).

3. The apparatus and its operation

3.1. Overview

The schematic of the calibration apparatus is shown in figure 1. The supplied air is at first divided into two lines; one to a getter dryer to generate zero-air (more details in section 3.3), and another one to the saturator. The air flows with equal temperature are then mixed and supplied to the measurement chamber. The inlet air humidity to the chamber is controlled by the mass flow rates and bath temperature. A small pressure reduction after the saturator ensures that condensation does not occur even if the flow rate through the getter dryer is zero. Prior to testing the performance of the whole apparatus, the saturator, zero-air heat exchanger, zero-air supply (getter dryer), pressure reducer and measurement chamber were tested separately. All the measuring devices included in the apparatus are calibrated at MIKES and their readings are traceable to SI.

3.2. Saturator

The saturator was designed to operate in single pressure mode because of easy usability, simple structure and low uncertainty. Saturators operating with the same principle are reported, e.g. in Mamontov (2000) and Zvizdic *et al* (2012). The saturator includes an inlet tube, a saturation chamber and a saturator heat exchanger. The inlet tube cools the gas close to saturation temperature and removes most of the excess water vapour. Direct contact with the ice/water surface in the saturation chamber ensures that the dew-point temperature of the air entering the saturator heat exchanger is slightly higher than the bath temperature. Full saturation is achieved in the saturator heat exchanger.

Pre-saturated air—in this case air with a higher dew-point temperature than the targeted dew-point temperature of the saturator—enters the saturator, where it cools down to the temperature of the bath and the excess water vapour is condensed. The output dew-point temperature of the air leaving the saturator is traceable to SI through temperature and pressure measurements. A photo of the saturator and all the components immersed in the bath is shown in figure 2.

To obtain the traceability of the generated dew-point temperature through temperature and pressure measurements we needed to characterize the saturation efficiency. If the air is fully saturated, the outlet dew-point temperature is independent of the flow rate.

For the experimental characterization of the saturation efficiency, the measurement chamber was replaced with a tube connected directly to an MBW373LX chilled mirror dew-point meter. Tests were carried out at the dew/frost-point temperatures of +10, −30 and −80 °C, at the flow rates of 0.6 l min^{-1} and 1.0 l min^{-1} and with different humidity levels at saturator inlet. Figure 3 shows the results of the flow tests at a saturator temperature of −80 °C. In the results during the first 3 h the flow rate was 1.0 l min^{-1}, which corresponds to the maximum flow rate of the MFC. Then (at the point of the first dashed line in figure 3) the flow rate was reduced to 0.6 l min^{-1} and at 6.7 h the flow rate was switched back to 1.0 l min^{-1}. The results show no flow dependency and also the repeatability of the generated dew-point temperature was within 0.01 °C. Thus, the assumption of 100% saturation efficiency is justified within an uncertainty of 0.01 °C. Similar results were obtained in the tests at different dew/frost-point temperatures. Additionally, the sensitivity of the dew-point temperature measurement to changes in the saturator temperature was studied by changing the bath temperature by 0.01 °C. The generated dew-point temperature followed the bath temperature by changing 0.01 °C.

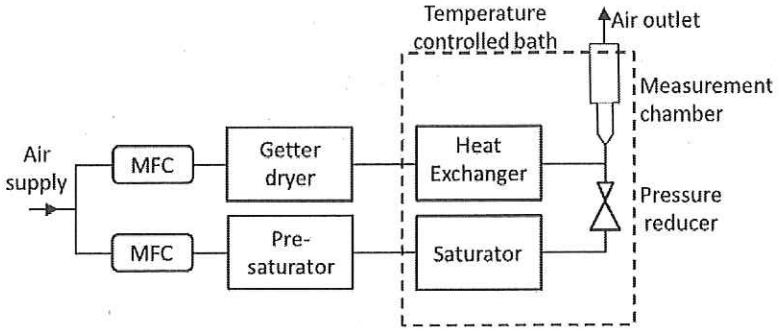

Figure 1. Schematic of the calibration apparatus. MFC denotes mass flow controller.

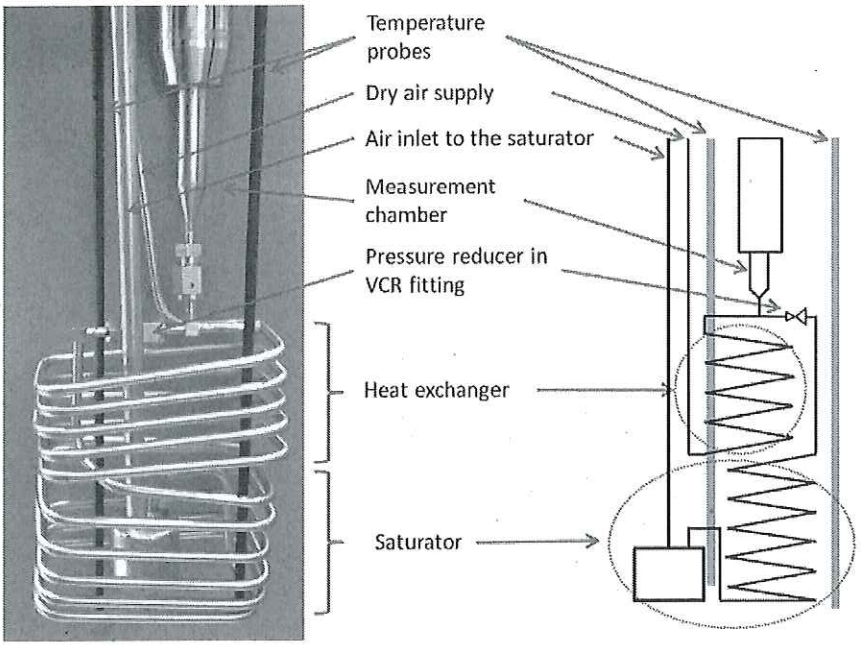

Figure 2. Heat exchanger, saturator, measurement chamber and temperature probes photographed on the left. On the right is a schematic of the same construction.

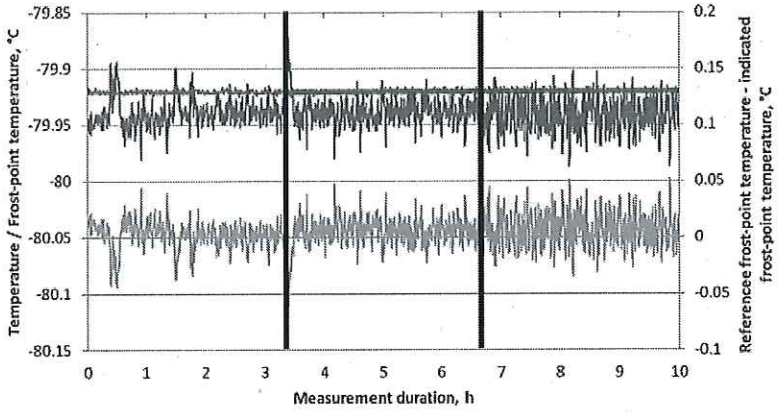

Figure 3. Results of the flow test for the saturator at −80 °C. The three plots starting from the top are the temperature of the saturator (left scale), the frost-point temperature indicated by the dew-point meter (left scale) and the pressure corrected frost-point temperature minus the dew-point meter indicated frost-point temperature (right scale). The flow rate at the beginning of the measurement and at the end was 1.0 l min^{-1} and between the dashed lines 0.6 l min^{-1}.

Additional evidence on the performance of the saturator was obtained by comparing the test results with the calibration of the chilled mirror hygrometer against the MIKES primary Dew/Frost-point Generator (MDFG). The results agreed well within the expanded uncertainties of the MDFG, i.e. 0.2 °C at −80 °C and 0.05 °C above − 60 °C ($k = 2$).

3.3. Zero-air supply

The term zero-air typically means dry air that contains nothing else but air. However, there is always some water vapour (trace moisture) as well as other components present. In this paper zero-air means air-dried with a MC400 getter manufactured by SAES Pure Gas Inc. The getter removes water molecules and decreases the dew-point temperature to approximately −90 °C.

Because the getter adsorbs water molecules its efficiency to remove water molecules decreases with time as the adsorption medium becomes saturated with water molecules. The humidity content of the air exiting the getter is regularly measured with a HALO trace gas analyser manufactured by Tiger Optics.

The air passing through the getter dryer is cooled down to measurement temperature prior to mixing and entering the measurement chamber. For the cooling, the air flows through a tube coil (zero-air) heat exchanger immersed in an ethanol bath. Thus, the air temperature in the outlet of the zero-air heat exchanger matches the temperature of the air coming from the saturator and the temperature of the ethanol in the bath. Because direct air temperature measurement in the coil was difficult to perform in a reliable way, the efficiency of the zero-air heat exchanger was tested by applying it as a saturator (by introducing air with a higher dew/frost-point temperature than the bath temperature to the zero-air heat exchanger and decreasing the outlet dew/frost-point temperature down to the bath temperature by condensation of excess water vapour in the zero-air heat exchanger) and comparing the output dew-point temperatures of the saturator and the zero-air heat exchanger. No flow dependency was detected with flow rates up to 1.0 l min^{-1} and thus it is justified to claim that the heat exchanger functions as designed.

3.4. Pressure reducer and air mixing

Radiosondes are calibrated in non-condensing conditions, i.e. at RH <100%. Furthermore, any condensation of water vapour after the saturator would be a significant potential source of error when operating with the calibration system. To ensure reliable operation and to enable measurements solely with the saturator, a small pressure drop is introduced in the outlet of the saturator. This was realized by a plugging seal with a hole of 1 mm diameter in a VCR® connection. This reduces the pressure by about 20 hPa depending on the flow volume through it. This is enough to ensure that no condensation occurs on the inner walls of the tubes or the measurement chamber. The effect of the pressure drop to the dew-point temperature is taken into account by pressure measurements.

Air mixing takes place in a Swagelok standard T-joint for an outer diameter of 6 mm tubes. The mixing ratio of the flows is controlled by two mass flow controllers (MFCs) placed prior to the saturator and the getter. Both controllers are Bronkhorst manufactured devices of model F-201C-RAA-33V.

3.5. Measurement chamber

The measurement chamber specially designed for radiosonde calibrations is presented in detail in (Lakka *et al* 2013) and (Sairanen *et al* 2014). The chamber consists of two parts: the actual measurement chamber for the sensor followed by another chamber for the sensor electronics. Internally the parts are separated from each other by a leaking seal. The high air speed through the seal minimizes the back-diffusion of water vapour from the second chamber to the actual measurement chamber. In figure 2 the chamber for the electronics is above the actual measurement chamber indicated by an arrow. By having the electronics in a different space than the sensor, this construction minimizes the inner volume of the actual measurement chamber. This enables a short stabilization time and quick response to changes in measurement parameters. As a result, the overall calibration time is significantly reduced to just a couple of days.

The actual measurement chamber is fully immersed in ethanol. However, the immersion of the chamber for the electronics is 5 cm, and its upper end is on the bath cover. Thus, the chamber wall conducts heat from the ambient to the actual measurement chamber and increases the temperature there, depending on the flow rate and bath temperature, at a maximum of 4 °C. When performing calibrations for radiosondes with heated humidity sensors this temperature increase does not cause any complication in the measurements. This kind of assembly allows the easy opening of the chamber without removing the chamber or any components, and thus makes it easy to change the radiosonde under calibration. This increases the usability of the calibration set-up.

3.6. Pressure measurements

As a gas flows, the resistance from the tube walls decreases the gas pressure. Because the water vapour pressure reduces with the reducing total gas pressure, the pressure drop has to be taken into account when determining the water vapour partial pressure or dew-point temperature in the measurement chamber. Thus, pressure measurements are an integral part of the operation of a humidity calibration system. However, dead space in the tubing of pressure measurements and water vapour permeation through the tube walls may affect the partial pressure of the water vapour in the system. In order to avoid these problems the pressure is measured only at the inlets of the saturator and the getter. The pressure resistance in the apparatus was characterized with different flow rates and ratios by measuring the pressures at the inlets and at the

Table 1. Summary of the uncertainty analysis of the outlet dew/frost-point temperature of the saturator.

Source	Probability distribution	Contribution to the combined standard uncertainty
Temperature deviation	Normal	0.0010 °C
Drift of the thermometer	Rectangular	0.0052 °C
Resolution of the thermometer	Rectangular	0.0006 °C
Calibration uncertainty of the thermometer	Normal	0.0040 °C
Temperature gradients	Rectangular	0.0115 °C
Saturation efficiency	Rectangular	0.0058 °C
Combined standard uncertainty		0.015 °C

Table 2. Uncertainty analysis of the complete apparatus for the mixing ratio at −80 °C in a case of an equally mixed flow.

Source	Estimate	Uncertainty of the input quantity	Sensitivity coefficient	Contribution to the standard uncertainty
Zero-air supply				
Frost-point temperature	183.15 K	0.25 K	-5.16×10^{-9} K^{-1}	-1.29×10^{-9}
Water vapour pressure[a]	9.67×10^{-3} Pa	2.9×10^{-5} Pa	3.02×10^{-6} Pa^{-1}	8.77×10^{-11}
Enhancement factor[a]	1.0085	1.01×10^{-3}	2.90×10^{-8}	2.92×10^{-11}
Pressure	10, 3800 Pa	20 Pa	-2.81×10^{-13} Pa^{-1}	-5.63×10^{-12}
Air flow rate	1.09×10^{-4} g s^{-1}	1.09×10^{-4} g s^{-1}	-6.23×10^{-6} s g^{-1}	-6.78×10^{-10}
Saturator				
Frost-point temperature[b]	193.15 K	0.015 K	-2.61×10^{-8} K^{-1}	-3.92×10^{-10}
Water vapour pressure[a]	5.47×10^{-2} Pa	1.64×10^{-4} Pa	3.01×10^{-6} Pa^{-1}	4.95×10^{-10}
Enhancement factor[a]	1.0076	1.01×10^{-3}	1.64×10^{-7}	1.65×10^{-10}
Pressure	10, 4000 Pa	20 Pa	-1.59×10^{-12} Pa^{-1}	-3.17×10^{-11}
Air flow rate	1.09×10^{-4} g s^{-1}	1.09×10^{-4} g s^{-1}	6.23×10^{-6} s g^{-1}	6.78×10^{-10}
Molar masses				
Water	18.02 g mol^{-1}	2.40×10^{-5} g mol^{-1}	1.08×10^{-8} mol g^{-1}	2.74×10^{-13}
Air	28.96 g mol^{-1}	2.55×10^{-5} g mol^{-1}	-6.70×10^{-9} mol g^{-1}	-1.71×10^{-13}
Adsorption/desorption	0	5.82×10^{-10}	1	5.82×10^{-10}
Standard uncertainty				1.83×10^{-9}
Relative standard unc				0.94%
Expanded uncertainty ($k = 2$)				3.66×10^{-9}
Relative expanded unc				1.89%

[a] Only the uncertainties of the formulae are considered here.
[b] See table 1.

measurement chamber inlet. By utilizing the pressure characterization data, the pressure at the point of interest is determined from the inlet air pressure. The pressure measurements are carried out with a PTB330 barometer manufactured by Vaisala. By utilizing electrically controlled valves only one barometer is used for all the pressure measurements.

3.7. Tests with the complete apparatus

To finalize the characterization of the apparatus, several tests with RR01 prototype reference radiosondes of Vaisala were performed for the complete set-up. Due to significant adsorption/desorption effects in the chamber for the sensor electronics, an external hygrometer was not used in these tests. The results show that the dew-point temperature in the actual measurement chamber with each set point is repeatable within the uncertainty of the RR01s. Also, changes in the mixing ratio resulted in corresponding changes in readings of RR01s, and none of the RR01s indicated flow dependency.

4. Uncertainty analysis

The test results for the apparatus described above were used for analysing the uncertainty of the generated water vapour mixing ratio in the measurement chamber according to JCGM (2008). A preliminary uncertainty budget for the apparatus was presented in (Lakka *et al* 2013), but it was based on theoretically determined design values for the performance of the saturator and a low temperature saturator (which was replaced by the getter dryer in this work). The summary of the uncertainty analysis in tables 1 and 2 represents the actual performance of the constructed system.

The uncertainty of the dew-point temperature generated by the saturator is mainly contributed by temperature measurements, temperature gradients and the efficiency of the saturator. Because the thermometer unit comprising two Pt 100 thermometers (Fluke 5609-20) and a digital multimeter Agilent 34970A is calibrated as a complete system, the calibration uncertainty includes contributions of self-heating and immersion depth. All key sources of uncertainty and their role in total uncertainty are shown in table 1.

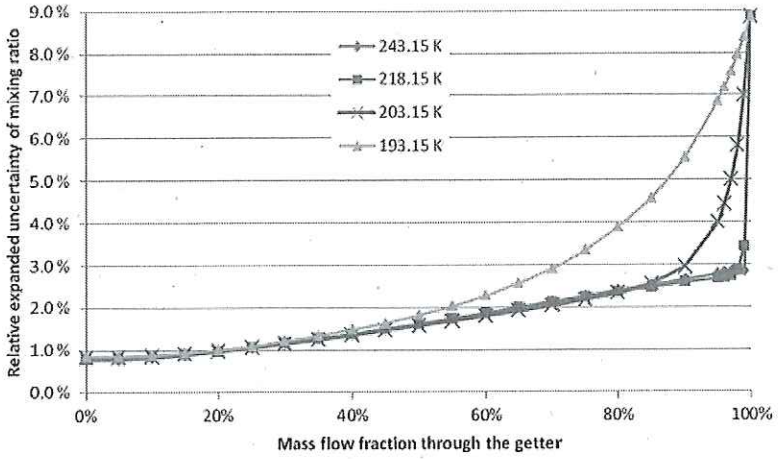

Figure 4. Relative expanded ($k = 2$) uncertainty of the mixing ratio as functions of mass flow fraction through the getter. The ▲, ×, ■ and ♦ symbols stand for the −80 °C, −70 °C, −55 °C and −30 °C temperatures of the measurement chamber, respectively.

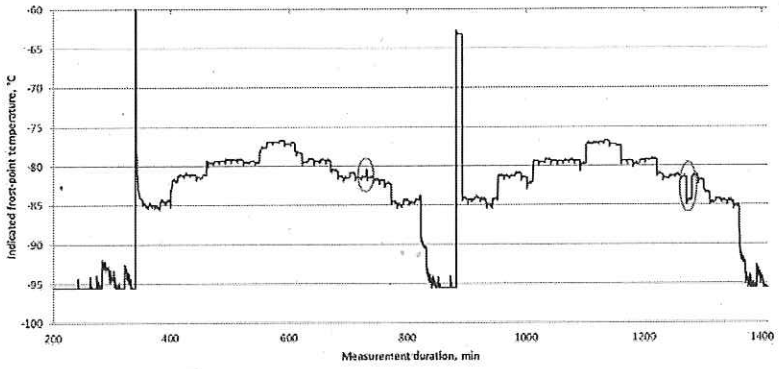

Figure 5. Recorded frost-point temperature readings of a prototype reference radiosonde RR01 of Vaisala's reference radiosonde programme during a test calibration at −80 °C. At the red ellipses a flow test, i.e. doubling the total flow rate while maintaining the same frost-point temperature, was carried out.

A conservative estimation was applied to the outlet dew-point temperature of the getter dryer because its capability to adsorb water vapour decreases slowly with time. In addition, the drying efficiency of the getter depends on the air flow rate through it and the air pressure. A safe estimate for the uncertainty of the getter used in this work is 0.25 °C.

An uncertainty budget for the complete apparatus, i.e. for the mixing ratio in the measurement chamber, is shown in table 2. It includes an uncertainty source of adsorption/desorption effects, which was estimated by time response measurements when switching dry air to a humid air flow.

The combined uncertainty of the mixing ratio depends on humidity, i.e. the flow rates of the dry and humidified air to be mixed as well as the temperature of the liquid bath. Table 2 presents only a single example at a selected temperature and flow rates. Figure 4 illustrates the relationship between the overall uncertainty and the system settings. The uncertainty values shown in the figure were calculated by keeping the flow rate through the measurement chamber constant, but varying the ratio of the flow rates through the getter and saturator. The results show that the uncertainty increases as the flow rate fraction through the getter increases. This is due to the large uncertainty contribution of the getter. Due to the exponential saturation water vapour curve, the derivates of the uncertainty curves increase rapidly when the mass flow fraction through the getter approaches 100%. The increase is more dramatic with a higher saturation temperature.

5. Test of the calibration procedure

To test the calibration procedure, several test calibrations were carried out for RR01s. The longest stabilization times are expected at the coldest temperature and the lowest water vapour concentrations. An example of a calibration measurement with set-points in terms of the mass flow fraction through the getter are of 100%, 67%, 50%, 33% and 0%, as shown in figure 5. The same set-points are used at every calibration temperature. The readings of an RR01 are in terms of dew-point temperature and thus the unit was chosen for figure 5.

In this test of the calibration procedure, a test measurement sequence was repeated twice, each including measurements of the set-points in both ascending and descending order. Before the first sequence, the system was allowed to stabilize to as dry

conditions as possible by flushing the system with air from the getter. At the set point of 50% in the set of descending humidity set points a flow test (i.e. common humidity calibration procedure to study the flow dependence of the device under calibration) was carried out in each measurement sequence. Although the flow rate ratio between the getter and the saturator was kept unchanged the total flow rate through the measurement chamber was doubled during the flow test to study the flow dependence of the device under calibration. These tests can be seen in figure 5 at 730 min and at 1270 min (marked with red ellipses). Ideally, the change in flow rates should cause no change in the dew-point temperature reading. However, adjustments to the MFC flow control may produce peaks in the humidity indication, because the pressure change corresponding to the flow adjustment disturbs the humidity level in the chamber. In figure 5 the peaks can be seen in the red ellipses.

Figure 5 demonstrates that a calibration of a radiosonde at a single temperature can be performed within 15 h. The figure also shows a very good repeatability of the RR01 and no hysteresis.

6. Discussion and conclusions

A new apparatus for radiosonde calibrations meeting GRUAN requirements was constructed and tested. The performance and potential for routine calibrations were analysed and demonstrated by a thorough validation including full uncertainty analysis and test calibrations. Our analysis shows that the expanded relative uncertainty of the mixing ratio in the measurement chamber ($k = 2$, confidence level of 95%) is 2% or less in the major part of the operating range, i.e. when the fraction of the zero air flow rate is less than 55%.

The test calibration shown in figure 5 demonstrates that the apparatus is capable of generating a stable frost-point temperature within 1 h even at the most challenging measurement points. This means that a full calibration at a single temperature can be carried out twice within 24 h. This is significantly shorter than that achievable with traditional humidity generators. Fast operation enables the system to be also used for characterizing the behaviour of radiosondes in changing temperatures and water vapour concentrations.

In the present configuration a getter dryer is used for providing zero air to be mixed with air saturated at the same temperature as the measurement chamber. In a future work, the getter will be replaced by a low frost-point saturator operating down to −90 °C. In this way, the uncertainty at low water vapour concentrations will be improved and the target uncertainty of 2% in the mixing ratio will also be achieved in the extreme range. Also, an interlaboratory comparison will be carried out to demonstrate the international equivalence of the developed system. The temperature homogeneity in the measurement chamber and the applicability of the set-up for vacuum pressures will be improved. Additionally, the suitability for different kinds of humidity sensors will be developed to improve the versatility of the system.

Acknowledgments

This work was supported by the European Metrology Research Programme (EMRP) jointly funded by the EMRP participating countries within EURAMET and the European Union. The authors are also thankful to Vaisala for providing RR01 reference radiosondes while testing the calibration apparatus.

References

GCOS 2007 *GCOS Reference Upper-Air Network (GRUAN): Justification, Requirements, Siting and Instrumentation Options* (Geneva: World Meteorological Organization)

GCOS 2013 *The GCOS Reference Upper-Air Network (GRUAN) GUIDE* (Geneva: World Meteorological Organization)

Hardy B 1998 ITS-90 formulations for vapour pressure, frostpoint temperature, dewpoint temperature, and enhancement factors in the range −100 to +100 °C *3rd Int. Symp. on Humidity and Moisture* vol 1, pp 214–22

JCGM 2008 *Evaluation of Measurement Data—Guide to the Expression of Uncertainty in Measurement*

Lakka A, Sairanen H, Heinonen M and Högström R 2013 Comsol-simulations as a tool in validating a measurement chamber *Presentation in Tempmeko 2013 (Madeira, Portugal)*

Mamontov G 2000 Application of the phase equilibrium method for generation of −100 °C of humid gas frost-point temperature *Meas. Sci. Technol.* **11** 818–27

Meyer C, Miller W, Ripple D and Scace G 2008 Performance and validation tests on the NIST hybrid humidity generator *Int. J. Thermophys.* **29** 1606–14

Sairanen H, Heinonen M, Högström R, Lakka A and Kajastie H 2014 A calibration system for reference radiosondes that meets GRUAN requirements *NCSLI Measure J. Meas. Sci.* **9** 56–60

Sonntag D 1998 The history of formulations and measurements of saturation water vapour pressure *3rd Int. Symp. on Humidity and Moisture* vol 1, pp 93–102

Wieser M 2006 Atomic weights of the elements 2005 (IUPAC Technical Report) *Pure Appl. Chem.* **78** 2051–66

Zvizdic D, Heinonen M and Sestan D 2012 New primary dew-point generators at HMI/FSB-LPM in the Range from −70 °C to +60 °C *Int. J. Thermophys.* **33** 1536–49